PERGAMON

Vision Research 40 (2000) 391–399

Vision Research

www.elsevier.com/locate/visres

Visual system's adjustments to illuminant changes: heuristic-based model revisited

J.L. Nieves *, J. Romero, J.A. García, E. Hita

Departamento de Óptica, Facultad de Ciencias, Universidad de Granada, 18071 Granada, Spain

Received 25 May 1999; received in revised form 13 August 1999

Abstract

This study evaluates the effect of illuminant changes along the two post-receptoral mechanisms: red–green ($L-2M$) and yellow–blue ($L+M-S$). By means of a CRT colour monitor, Mondrian-type scenes were simulated and a series of asymmetric colour matches were made with five test illuminants. The standard objects comprising the scenes were simulations of surfaces under equal-energy illuminant and were selected according to lines of equal excitation of the red–green and the yellow–blue mechanisms. Results show that observers' matches are well predicted by assuming affine transformations between test and standard illuminant conditions. The best linear fits derived from the data corroborates the previous heuristic-based algorithms [Zaidi Q. (1998) *Journal of the Optical Society of America A*, *7*, 1767–1776] although some discrepancies were found. Results along red–green mechanism confirm that the significant effect of the illuminant is an additive change along this axis, while data for yellow–blue mechanism suggest that illuminant induces not only multiplicative changes along this axis but additive too. In addition, we found that memory factors involved in the experiment could influence the observers' matches and would be taken into account as responsible of the differences found between the yellow–blue and the red–green systems.

Keywords: Colour vision; Colour constancy; Asymmetric matching; Opponency; Adaptation

1. Introduction

Colour constancy is traditionally defined as the perceived stability of the colour of objects with independence of the spectral composition in the surrounding illumination (Pokorny, Shevell & Smith, 1991). Although experimental studies on colour constancy have proliferated in recent years, few works systematically measure this perceived stability in the colour appearance at opponent stages (Brainard & Wandell, 1992; Lucassen & Walraven, 1993; Bäuml, 1994, 1995; Wei & Shevell, 1995; Brainard, Brunt & Speigle, 1997; Zaidi, Spehar & DeBonet, 1997). Rather, most works have focused on developing colour-constancy models assuming implicitly that this phenomenon occurs in a perfect manner, leading these models to find a stable representation of object colour independently of the variable illuminant conditions. Although discounting illuminant changes completely can be highly useful in automatic systems of colour analysis and synthesis (Maloney & Wandell, 1986; Wandell, 1987; D'Zmura & Iverson, 1993), the use of any algorithm for artificial vision should take into account that human visual system does not exhibit perfect colour constancy.

Recent heuristic-based models have shown that chromaticities of natural objects change in a different way along red–green and yellow–blue dimensions: illuminant changes, for different phases of natural daylight, lead to an additive change along the first dimension and a multiplicative change along the second one (Zaidi, 1998). This result can be used to simplify the colour-constancy algorithms since all that is required is to retain the invariant colour of the objects, e.g. object descriptors that remain invariant under different illuminant conditions. The key of the heuristic analysis is to consider that changes in the perceived colour under different illuminant conditions can be used not only to identify illuminants but also objects across illuminants.

* Corresponding author. Tel.: +34-958-246367; fax: +34-958-248533.

E-mail address: jnieves@ugr.es (J.L. Nieves)

0042-6989/99/$ - see front matter
PII: S0042-6989(99)00183-2

These considerations changes the notion of colour constancy since it is the lack of perfect colour constancy which permits the visual system extracts information about the illuminant, the imperfection of this phenomenon being not a limitation of the visual system but a design feature.

The purpose of the present experiment is: (i) to examine the visual system's adjustment to illuminant changes and their effects at the opponent stages; and (ii) to test whether these effects can be well interpreted by assuming some invariant transformations at opponent stages. To do this, we have developed a set of asymmetric colour matches in which different objects are matched under five illuminant conditions. The standard objects to be matched are situated over lines of equal excitation of the red–green ($L-2M$) and the yellow–blue ($L+M-S$) mechanisms. The results are analysed in the cone-excitation space and modelled along the red–green and yellow–blue dimensions in order to test affine-invariant properties of colour mechanisms. To do this, we have used the model proposed by Zaidi (1998) which develops specific invariant properties of opponent signals under different illuminant conditions. Although other more sophisticated colour constancy algorithms (Maloney & Wandell, 1986; Forsyth, 1990; D'Zmura & Iverson, 1993) have been proposed, most of them require additional information about the scene such as the election of a reference white, or the use of validated basis functions. The use of affine invariant properties of colour signals at opponent stages permit to obviate these assumptions and identify objects and illuminants in the scene following an easier experimental procedure. Because there is sufficient evidence for both scaling on receptors and scaling on post-receptoral stages (Bäuml, 1995; Webster & Mollon, 1995; Brainard et al., 1997; Zaidi et al., 1997; Bäuml, 1999), our aim is not to refute one of these possibilities. The heuristic-based approach is an easier and faster algorithm to analyse the human colour constancy since it does not need any additional assumption on receptoral stages (e.g. scaling cone responses) and directly evaluates the colour signals at opponent stages.

2. Experimental method

2.1. Apparatus and calibration

The objects were presented on a Samsung CSD5577 Multisync CRT 15'' colour monitor controlled by an 8-bit per gun TigaStar graphic card installed in a computer. The monitor was calibrated using a Spectrascan PR-704 spectroradiometer from Photo Research. The spectroradiometer was positioned 1 m away and perpendicular to the screen. The calibration was based on accepting the spatial-independence hypothesis with a simple scale factor and independence of the phosphors (Cowan & Rowell, 1986; Brainard, 1989; Lucassen & Walraven, 1990). To ensure stable functioning conditions, we fixed certain positions of brightness and contrast dials, to maintain the assumption of independence of the phosphors (Díaz, Jiménez, Hita & Jiménez del Barco, 1996). These positions were chosen for the blue gun to have a luminance maximum within the photopic level of 16.0–20.0 cd/m^2. Nevertheless, in the calibration the constancy of the phosphors was not assumed as a working hypothesis (Jiménez del Barco, Díaz, Jiménez & Rubiño, 1995). Based on this protocol, we calculated the chromaticity coordinates of any stimulus generated on the screen, using the relationship between the DAC values (r_{DAC}, g_{DAC}, b_{DAC}) and the (X,Y,Z)-tristimulus values in the CIE-1931 colour space. To determine the gun positions that would allow us to generate a stimulus (X,Y,Z) from the calibrated data, we ran a computer program iteratively to find the stimulus closest to the one sought, taking into account a certain tolerance lower than the expected differential threshold. Because the emission of the phosphors deteriorates with time, the calibration was repeated periodically (Jiménez del Barco et al., 1995).

2.2. Spatial configuration, objects, and illuminants

The spatial configuration of the objects in the CRT monitor screen consisted of a structure containing 34 randomly arranged different geometric shapes of flat colours, creating a Mondrian-type image. This image was presenting as an $11.2° \times 14.2°$ pattern of visual angle. During the session, the observer viewed successively an adaptive and a Mondrian-type background, the observer's sight being fixed at the central area of the screen. Through the matching phase, this area retained its position and size ($1.7° \times 1.7°$ of visual angle), as opposed to the rest, which changed randomly in terms of geometry and position on the screen. The randomness of the position and shape of the stimuli comprising the background avoided after-image interference during the adaptation period. In this way, we ensured that the observer did not perform the match by using some object on the screen as a reference, as described by other authors in similar experiments (Arend & Reeves, 1986; Cornelissen & Brenner, 1995).

Each object was described in terms of its reflectance function $S(\lambda)$ according to a linear model, which were based on the first three vectors of the Parkkinen basis (Parkkinen, Hallikainen & Jaaskelainen, 1989). In this way, the reflectance of any object of the scene was expressed as the linear combination:

$$S(\lambda) = \sum_{j=1}^{3} \sigma_j S_j(\lambda) \tag{1}$$

where S_j are the basis vectors and σ_j its corresponding weights on that basis. With a known spectral-power distribution of the illuminant $E(\lambda)$, as well as the chromaticity coordinates and luminance of the object under this illuminant, we could calculate its σ_j coordinates (see Troost & Weert, 1992, pp. 317–318, for full details). Finally, replacing these values in Eq. (1), the reflectance function $S(\lambda)$ of the objects was completely specified as well as its new coordinates under any other test illuminant.

The group of object colours used in the different experimental sessions were split into two well-differentiated groups: the *standard object colours*, which simulated object colours under the reference illuminant; and the *test object colours*, which comprised each Mondrian background under the different test illuminants. For the standard object colours, we chose 16 objects that were reproduced under the equal-energy illuminant. These objects were situated over four tritanopic confusion lines (yb lines), where only the excitation level of the S cones varied, and over six equal-excitation lines of the S cones (rg lines), where the excitation of the cones L and M were of opposing character. The luminance of all the stimuli was 22.0 cd/m^2. The objects were chosen according to two axes in the cone-excitation space proposed by Boynton (1986). The abscissa axis is identified in this space with the excitation of the red–green opponent mechanism — defined as $L-2M$ — while the ordinate axis corresponds to the excitation of the yellow–blue opponent mechanism — defined as $L+M-S$. The diagram in Fig. 1 represents a constant luminance plane, defined within the model as $L+M$. The values of L, M and S were based on the fundamentals proposed by Smith and Pokorny (1975), and were expressed in units of retinal illumination or troland (De Groot & Gebhard, 1952) in such a way that the luminance of the stimuli remained fixed at 144 td. This level of luminance was chosen in order to maintain the linear and additive behaviour of the guns and to ensure stable functioning conditions.

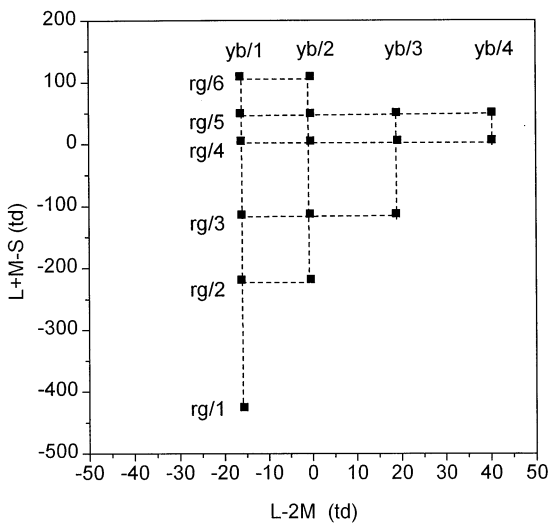

Fig. 1. Coordinates of the standard object colours chosen over different tritanopic confusion lines (yb lines) and over lines of constant stimulation of the S cones (rg lines), in the cone-excitation space proposed by Boynton (1986).

The test object colours were comprised of 34 objects making up the Mondrian-type background. These objects were distributed uniformly throughout the chromaticity diagram, thereby simulating the variety of different stimuli that habitually made up a real scene. The mean luminance of all test objects was close to but not exceeding 22.0 cd/m^2. This minimises the possibility that the background could have additional inductive effects on the observer's matches, given that in these kind of tasks where memory is involved, it is possible to find an increasing trend in luminance in relation to the initially observed stimulus (Newhall, Burnham & Clark, 1957).

To have a broad group of illuminant conditions that would simulate the different colour appearances of objects, we used five test illuminants: an equal-energy illuminant, characterised by a flat spectral-power distribution; a 10 000 K-illuminant, representing the radiation of the black body at 10 000 K; a D_{65}-illuminant, representing a daylight phase with a correlated colour temperature of 6500 K; a F_{11}-illuminant as representative of a fluorescent-type illuminant (Colorimetry, Pub. CIE, 1986); and an A-illuminant, representing the radiation of the black body at 2856 K and taken as standard of the spectral emission of an incandescent lamp at this temperature.

2.3. Experimental method

The observational distance was set at 1 m (maximum visual angle of 14.2° × 11.2°). An isolation chamber painted black enabled the screen to be isolated from possible parasite light. The observer consistently made the matches with binocular vision and natural pupil. Although the standard and test objects were in all cases presented in such a way as to illuminate the same retinal zone (foveal vision) the character of the observations themselves enabled the observer at certain moments to scan the entire screen. This type of experimental design falls within a category of asymmetric colour matching, in which the standard and test stimuli are matched within different visual contexts. Each observer was asked to disregard the variations in the illuminant conditions and match the appearance of the object colour previously observed. In this way, as noted by Brainard and Wandell (1992), these asymmetric matches were not therefore matches by photopigment absorption, but rather were established at some point in the visual route in order to discount the illuminant.

At the beginning of each session, observers were dark adapted for 3 min followed by another 3 min of adaptation to a uniform achromatic background with the equal-energy chromaticity and 18.8 cd/m^2 of luminance. The observers' attention was maintained with a red fixation point that indicated the position to be occupied by the standard object colour. After this adaptation time, the observer fixated the standard object for 10 s. This object was embedded in a Mondrian-type background illuminated by the equal-energy illuminant. During this phase, observers were asked to memorise the colour appearance of the object under the reference illumination.

After this initial phase, the observer adapted to a test illuminant condition for 1 min. At this point, the observer's matching task began over a new Mondrian-type background. The test-matching zone was initially black. The observer had six buttons available in the keyboard to increase or diminish by one unit the DAC values of the red, green, and blue guns of the monitor, each separately. Two additional buttons were used for brightness control. Although there was no time limit to perform the matches, we requested less than 2 min after which, if not finished, the observers could cancel the match. During the matching task, the objects comprising the Mondrian-type background could randomly change shape and position to minimise chromatic induction over the matching zone. Observers were requested to match the previously viewed object according to a surface-match criterion (Arend & Reeves, 1986; Arend, Reeves, Schirillo & Goldstein, 1991; Cornelissen & Brenner, 1995). After the observers completed a match, there was an adaptation period of 1 min to an equal-energy background before beginning a new match. During an experimental session, lasting about 35 min, 40 colour matches were performed — eight standard colour objects under five test illuminants; each stimulus was matched five times and the average value taken. Observers made 80 colour matches corresponding to the 16 standard object colours and one test illuminant (then, we managed $16 \times 5 \times 5 = 400$ different colour signals per observer).

2.4. Observers

Three observers were used (JR, JA, and FP). All were corrected to normal acuity and had normal colour vision according to usual colour tests.

2.5. Model

The model we test is based on the heuristic analysis derived from Zaidi's (1998) results. The model predicts the effect of illuminant changes on second-stages (red–green or RG-signal, and yellow–blue or YB-signal) according to the following transformations,

$$\begin{aligned} \mathrm{RG_t} &= \alpha_{\mathrm{te}} + \mathrm{RG_e} \\ \mathrm{YB_t} &= \beta_{\mathrm{te}} \mathrm{YB_e} \end{aligned} \qquad (2)$$

where α_{te} and β_{te} are parameters of the model describing the chromaticity shifts between the test- and the equienergy-illuminant conditions along the red–green and the yellow–blue dimensions. The transformation is based on the correlation shown by the three cone-class responses leading to an additive change along the red–green mechanism and a multiplicative change along the yellow–blue one. The model permits the identification of objects under different illuminant conditions by the following procedure: the parameters α_{te} are evaluated as the average difference for all the objects comprising a scene between the red–green signal for one test illuminant and the corresponding red–green one for the equienergy illuminant; similarly, the parameters β_{te} are estimated as the average ratio for the same set of objects between the yellow–blue signal for one test illuminant and the corresponding one for the equienergy illuminant.

3. Results and discussion

Results derived from one observer's matches are presented in Fig. 2 for (a) the red–green and (b) the yellow–blue mechanism separately for each of the test illuminants. The reference excitation values, which were derived from the hypothesised surface reflectance and the equienergy illuminant, are presented on x-axis, while the obtained values derived from observer's matches under the test illuminant are presented on y-axis. From these figures we can see that illuminant changes lead to different kinds of transformations along red–green and yellow–blue axes. On one hand, results along RG axis are clustered along unity-slope lines (dashed lines in the figures), and on the other, results along YB axis suggest that observer's matches are distributed in a different way along the predicted values. These results corroborate the previous ones derived from heuristic considerations with different phases of daylight (Zaidi, 1998) and would support the use of the affine nature of the correlation at post-receptoral stages to identify illuminant changes.

The model predictions, as evaluated by Eq. (2), are also shown in the figures as open symbols. The obtained predictions describe fairly well data from red–green excitations, with a great coincidence between matches and predicted values. However, some discrepancies appear when yellow-blue excitations are considered. For this mechanism data deviate from theoretical predictions depending on both the illuminant and the excitation values of the mechanism. Greatest deviations occur for 10 000 K-illuminant, and the differences are accentuated when high-negative val-

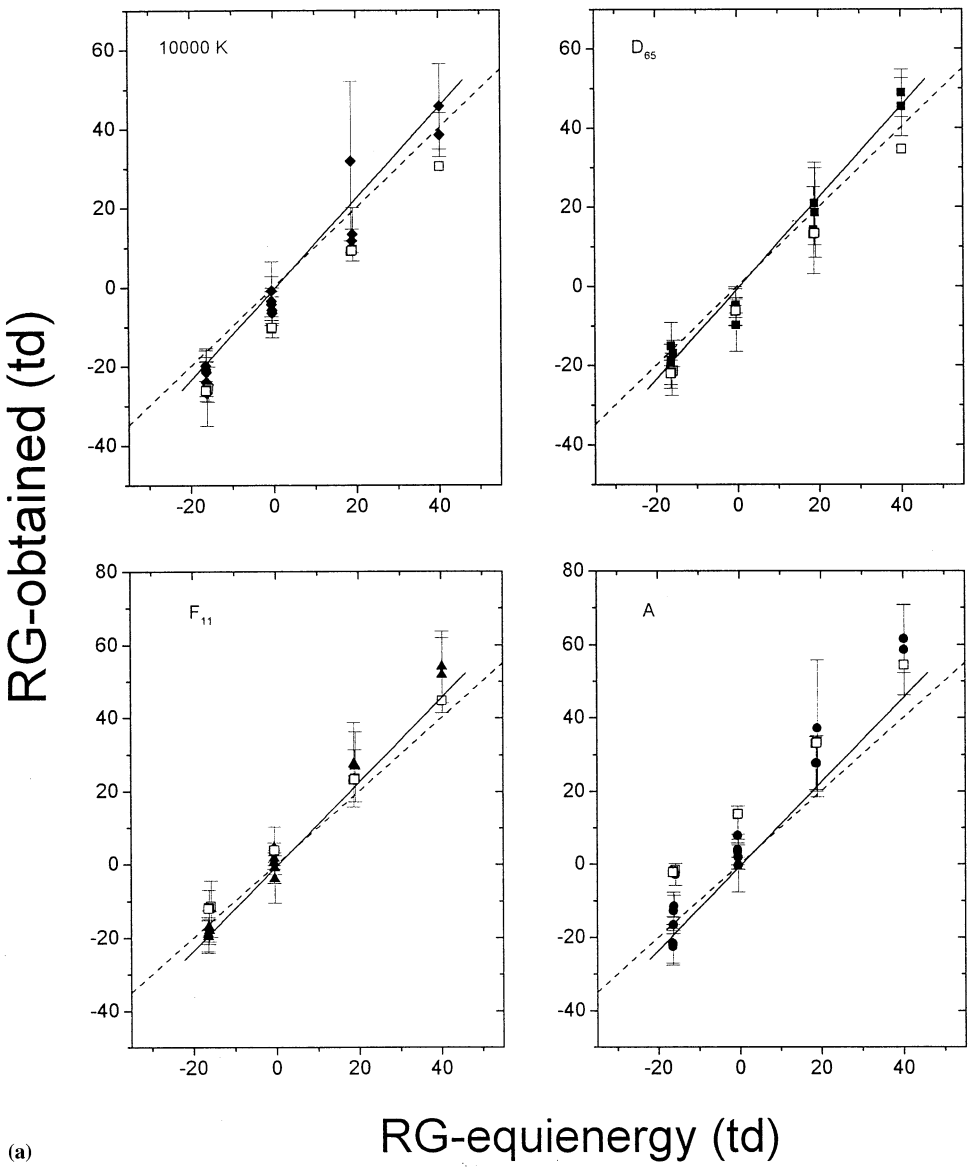

Fig. 2. Red–green excitations (RG) derived from the hypothesised surface reflectance under the equienergy illuminant (on x-axis) and the obtained from each of the test illuminants (on y-axis). Solid symbols are for observer's matches, and open symbols are for predictions derived from heuristic-based analysis (Zaidi, 1998); solid lines represent the best linear fits obtained for matches made without illuminant changes. Results are for observer JR. Each error bars represent ± 1 S.E. (b): Yellow–blue excitations (YB) derived from the hypothesised surface reflectance under the equienergy illuminant (on x-axis) and the obtained from each of the test illuminants (on y-axis). Solid symbols are for observer's matches, and open symbols are for predictions derived from heuristic-based analysis (Zaidi, 1998); solid lines represent the best linear fits obtained for matches made without illuminant changes. Results are for observer JR. Each error bars represent ± 1 S.E.

ues of YB excitation are considered. A possible explanation for these differences could be originated from the intrusion of memory factors in the experiment, which were derived from the degradation of the object retained in memory during intermediate adapting periods. These factors have been included in the figures as linear fits of the data (solid lines) derived from observer's matches when no illuminant change took place. Results suggest that that memory does not influence red-green excitations since linear fits almost coincide with the equienergy predictions (dashed lines). On the contrary, memory seems to be relevant when yellow–blue excitations are considered especially for negative values of YB excitation. The linear fits of the observer's matches made without illuminant change show a slope of 1.14 for the RG axis with an offset of -0.62, and a slope of 0.79 for the YB axis with an offset of 8.71. In this sense, the present experiment is not definitive and should be matter of a further analysis to draw more firm conclusions.

From the results of Fig. 2, specifically those ones obtained for the yellow–blue mechanism, we next

analyse with a more detail the linear fits which can be derived from our data. Since they correspond to standard objects along equal-excitation lines either of the yellow–blue (rg lines) or the red–green (yb lines) mechanisms, we can extent the analysis of Eq. (2) separately for each visual mechanism. From the above results, and permitting not only multiplicative changes along YB axis but additive too, we could use a more relaxed version of Eq. (2) to model the data obtained in the following form,

$$RG_t = \alpha_{te} + a_{te} RG_e$$

$$YB_t = b_{te} + \beta_{te} YB_e \quad (3)$$

If the only significant effect of the illuminant changes were an additive shift of the chromaticity of the objects along the red–green axis and a multiplicative shift along the yellow–blue axis, parameter a_{te} should take unity values while parameter b_{te} should be zero for all test illuminants considered. To examine more thoroughly these effects, we obtained the best linear fits of observer's matches, separately, for each of the rg and yb lines. For example, if we take the objects along the rg/4 line, we manage 20 colour signals (four objects × five matches per object) for each of the test illuminants to get the linear fit, e.g. slope of 1.04 and ordinate of -4.69 ($r = 0.98$) when 10 000 K-illuminant were used. The results are summarised in Table 1, which shows whether the effect of an illuminant change in the parameters a_{te} and b_{te} is significantly different from unity or zero, respectively, and their relative importance with respect to the average variations of α_{te} and β_{te} parameters.

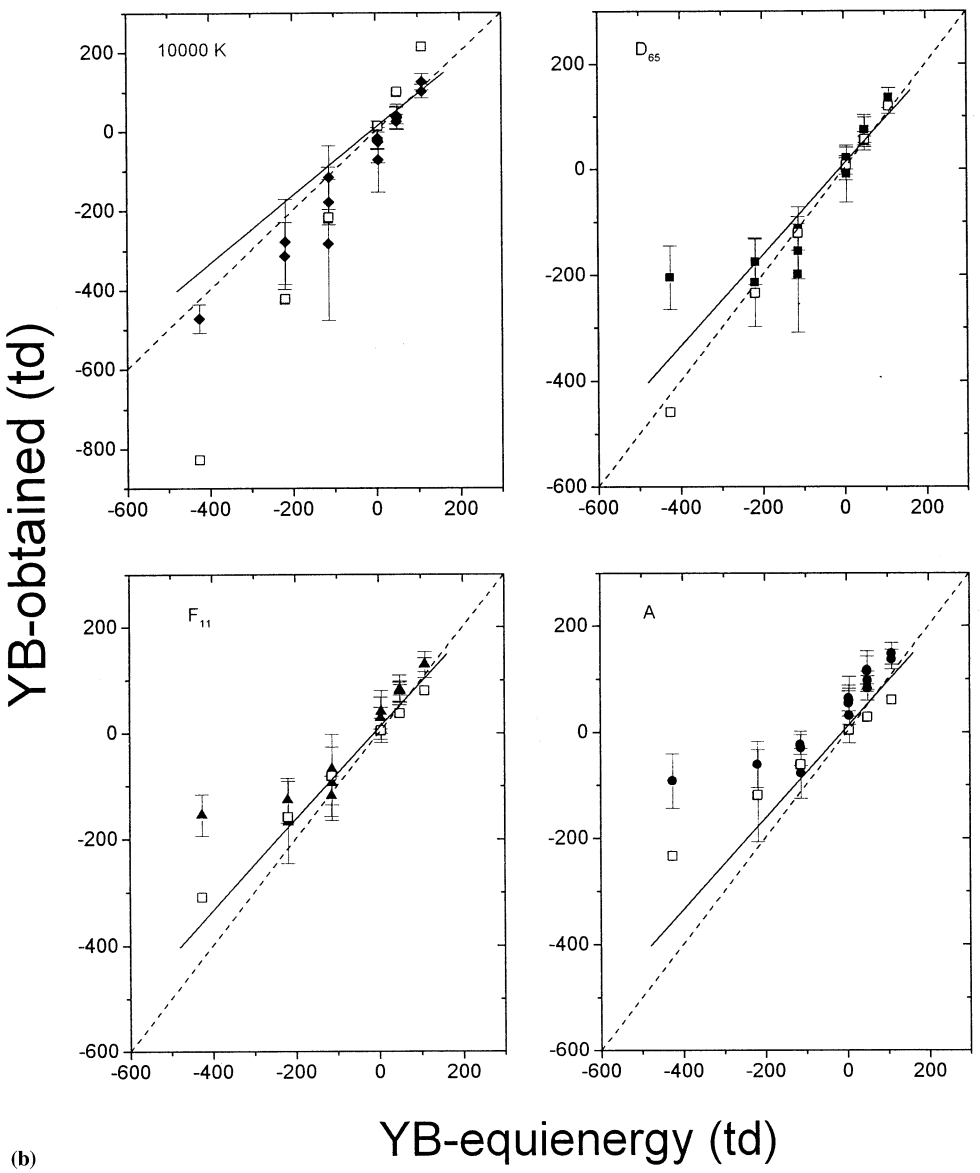

(b)

Fig. 2. (*Continued*)

Table 1
Best linear fit parameters and regression coefficients (r-values) as derived from linear scaling on post-receptoral (red–green and yellow–blue) mechanisms[a]

	Lines	α_{te}	a_{te}	r	Lines	b_{te}	β_{te}	r
10 000 K	rg/2	−0.25	1.46	0.90	yb/1	−42.21	1.14	0.91
D_{65}		−4.67	0.88	0.91		0.51	0.69	0.80
F_{11}		5.04	1.08	0.90		27.62	0.56	0.87
A		8.43	1.31	0.86		71.18	0.47	0.89
10 000 K	rg/3	−0.71	1.68	0.90	yb/2	−31.22	1.18	0.94
D_{65}		−5.20	1.03	0.92		2.34	0.98	0.94
F_{11}		2.30	1.29	0.94		25.08	0.94	0.93
A		5.69	1.12	0.96		50.33	0.86	0.91
10 000 K	rg/4	−4.69	1.04	0.98	yb/3	−19.31	0.91	0.76
D_{65}		−0.97	1.16	0.96		4.14	1.09	0.88
F_{11}		2.80	1.26	0.97		34.65	0.92	0.84
A		6.08	1.37	0.94		50.53	0.71	0.90
10 000 K	rg/5	−4.52	1.15	0.97	yb/4	−87.61	2.38	0.71
D_{65}		−2.20	1.17	0.97		15.99	0.69	0.79
F_{11}		0.94	1.27	0.98		−4.62	1.64	0.89
A		1.84	1.45	0.98		21.79	1.48	0.72
10 000 K	rg/6	−6.14	0.83	0.82				
D_{65}		−9.53	0.75	0.79				
F_{11}		−3.63	0.94	0.83				
A		0.14	1.38	0.89				

[a] Data are presented separately for each test illuminant, and for each of critical axis selected. See text for full details.

As we can see from Table 1, the individual analysis for each rg line shows that in some cases slopes values a_{te} of the best linear fits are close to unity. In addition, the values of the ordinate α_{te} change abruptly for all the rg lines, which suggest that the major effect of the illuminant is an additive change along the red–green mechanism. The average deviation from 1 for a_{te} is 0.18 (with a relative small standard deviation of 0.23), and the average value for α_{te} is -0.46 (with a large standard deviation of 4.69). This result confirms the above predictions derived from Eq. (2). On the contrary, best linear fits for the yb lines reveal that the test illuminants induce not only multiplicative changes but also additive too along the yellow–blue mechanism. As expected from the above discussion, we obtained important variations of parameter β_{te}, which are indicative of the multiplicative changes already mentioned. However, the obtained average values for b_{te} are significantly different from zero for each of the yb line considered, and cannot be only explain from heuristic-based predictions (Zaidi, 1998). The average value for b_{te} is 7.45 (with a large standard deviation of 39.53) and the average value for β_{te} is 1.04 (with standard deviation of 0.47) reflect the tendency. All of these effects are better predicted (high obtained r-values) when we consider lines comprising a large number of colour objects; as a matter of fact, poor fits were derived for lines comprising only two objects (i.e. rg/6 line and yb/4 line).

The 'different' responses associated to the colour-vision mechanisms at opponent stages are in agreement with other algorithms (Lucassen & Walraven, 1993) which are based on constant colour-contrast relations at receptoral stages, the only difference being the non linear functional form derived from them. Can we extrapolate these non-linearities to our results along the yellow–blue axis? If so, we need a more specific study to evaluate whether the discrepancies we found for the yellow–blue system depend on the illuminant conditions or are inherent to the signals derived from its excitation, making the yellow–blue mechanism different from the red–green with respect to colour-constancy experimental paradigms (Nieves, García-Beltrán & Romero, 1999). Other possibilities to be considered are, on one hand, the intrusion of memory factors in the experiment (see solid lines in Fig. 2). Our results confirm the previously ones found by Jin and Shevell (1996) showing that colour memory is more accurate on the L/M dimension than on the S dimension. We can expect a similar influence of memory when yellow–blue excitation $L+M-S$ is considered and, then, the non-zero values of b_{te} parameter shown in Table 1 would reflect this tendency. On the other, a possible explanation could also derived from the influence of the luminance term $L+M$ in the definition of the yellow–blue mechanism. Although luminance variations of the Mondrian surrounds objects were of little importance, it would be possible that the deviations obtained from Eq. (2) were originated by small changes in the overall luminance background. We cannot develop whether this is a plausible hypothesis or not with our experi-

ment and should be a further matter of study. In addition, more recent colour-vision models have reconsidered this aspect in the definition of the yellow–blue signal (De Valois & De Valois, 1993), so that the relevant role in the yellow-blue mechanism could be mediated more by the L- and M-cone excitations than by the S-cone system.

4. Conclusions

The main conclusions drawn form this study are that (i) experimental results support affine transformations based on additive and multiplicative changes along red–green and yellow–blue mechanisms, and (ii) identification algorithms based on these transformations should take into account variations of the predicted values depending on the excitation level of the colour-vision mechanisms. This is especially pronounced for the yellow–blue mechanism, for which we find the greatest variations between predicted and obtained values. In this case, good correlation is found when an additional constant is included in Eq. (2) derived from heuristic-based analysis (Zaidi, 1998). With respect to the $L-2M$ mechanism, results derived from observers' matches show that the significant effect of variable illuminant conditions is an additive change along this axis. This confirms the results derived from heuristic-based model predictions (Zaidi, 1998) and corroborates the previous ones derived with a different colour-constancy experimental paradigm (Zaidi et al., 1997).

Acknowledgements

This research has been supported by the Comisión Interministerial de Ciencia y Tecnología (CICYT), Spain, under grant PB96-1454.

References

Arend, L. E., & Reeves, A. (1986). Simultaneous color constancy. *Journal of the Optical Society of America A*, *3*, 1743–11751.

Arend, L. E., Reeves, A., Schirillo, J., & Goldstein, R. (1991). Simultaneous color constancy: papers with diverse Munsell values. *Journal of the Optical Society of America A*, *8*, 661–672.

Bäuml, K.-H. (1994). Color appearance: effects of illuminant changes under different surface collections. *Journal of the Optical Society of America A*, *11*, 531–542.

Bäuml, K.-H. (1995). Illuminant changes under different surface collections: examining some principles of color appearance. *Journal of the Optical Society of America A*, *12*, 261–271.

Bäuml, K.-H. (1999). Simultaneous color constancy: how surface color perception varies with the illuminant. *Vision Research*, *39*, 1531–1550.

Boynton, R. M. (1986). A system of photometry and colorimetry based on cone excitations. *Color Research and Application*, *11*, 244–252.

Brainard, D. H. (1989). Calibration of a computer controlled color monitor. *Color Research and Application*, *14*, 23–34.

Brainard, D. H., Brunt, W. A., & Speigle, J. M. (1997). Color constancy in the nearly natural image. I. Asymmetric matches. *Journal of the Optical Society of America A*, *14*, 2091–2110.

Brainard, D. H., & Wandell, B. A. (1992). Asymmetric color matching: how color appearance depends on the illuminant. *Journal of the Optical Society of America A*, *9*, 1433–1448.

CIE Publication, 1986. Colorimetry, no 152, CIE Central Bureau.

Cornelissen, F. W., & Brenner, E. (1995). Simultaneous colour constancy revisited: an analysis of viewing strategies. *Vision Research*, *35*, 2431–2448.

Cowan, W. B., & Rowell, N. (1986). On the gun independence and phosphor constancy of colour video monitors. *Color Research and Application*, *11*, 533–538.

D'Zmura, M., & Iverson, G. (1993). Color constancy. I. Basic theory of two-stage linear recovery of spectral descriptions for lights and surfaces. *Journal of the Optical Society of America A*, *10*, 2148–2165.

De Groot, S. G., & Gebhard, J. W. (1952). Pupil size as determined by adapting luminance. *Journal of the Optical Society of America*, *42*, 492–495.

De Valois, R. L., & De valois, K. K. (1993). A multi-stage color model. *Vision Research*, *33*, 1053–1065.

Díaz, J. A., Jiménez, J. R., Hita, E., & Jiměnez del Barco, L. (1996). Optimizing the constant-channel chromaticity and color gamut of CRT color displays by control of brightness and contrast level. *Applied Optics*, *35*, 1711–1718.

Forsyth, D. (1990). A novel algorithm for color constancy. *International Journal of Computer Vision*, *30*, 5–36.

Jiménez del Barco, L., Díaz, J. A., Jiménez, J. R., & Rubiño, M. (1995). Considerations on the calibration of CRT color displays assuming constant channel chromaticity. *Color Research and Application*, *20*, 377–387.

Jin, E. W., & Shevell, S. K. (1996). Color memory and color constancy. *Journal of the Optical Society of America*, *A*, *13*, 1981–1991.

Lucassen, M. P., & Walraven, J. (1990). Evaluation of a simple method of color monitor recalibration. *Color Research and Application*, *15*, 321–326.

Lucassen, M. P., & Walraven, J. (1993). Quantifying color constancy: evidence for nonlinear processing of cone-specific contrast. *Vision Research*, *33*, 739–757.

Maloney, L. T., & Wandell, B. A. (1986). Color constancy: a method for recovering surface spectral reflectance. *Journal of the Optical Society of America A*, *3*, 23–33.

Newhall, S. M., Burnham, R. W., & Clark, J. R. (1957). Comparison of successive with simultaneous color matching. *Journal of the Optical Society of America*, *47*, 43–56.

Nieves, J.L., García-Beltrán, A., Romero, J. (1999). Response of the human visual system to variable illuminant conditions: an analysis of opponent-color mechanisms in color constancy. Ophthalmic and Physiological Optics (in press).

Parkkinen, J. P. S., Hallikainen, J., & Jaaskelainen, T. (1989). Characteristic spectra of Munsell colors. *Journal of the Optical Society of America A*, *6*, 318–322.

Pokorny, J., Shevell, S. K., & Smith, V. C. (1991). Colour appearance and colour constancy. In P. Gouras, *The Perception of Colour* (pp. 43–61). London: Macmillan.

Smith, V. C., & Pokorny, J. (1975). Spectral sensitivity of the foveal cone photopigments between 400 and 500 nm. *Vision Research*, *15*, 161–171.

Troost, J. M., & Weert, C. M. M. (1992). Techniques for simulating object colors under changing illuminant conditions on electronic displays. *Color Research and Application*, *17*, 316–327.

Wandell, B. A. (1987). The synthesis and analysis of color images. *IEE Transactions on Pattern Analysis and Machine Intelligence*, *9*, 2–13.

Webster, M. A., & Mollon, J. D. (1995). Colour constancy influenced by contrast adaptation. *Nature*, *373*, 694–698.

Wei, J., & Shevell, S. K. (1995). Color appearance under chromatic adaptation varied along theoretically significant axes in color space. *Journal of the Optical Society of America A*, *12*, 36–46.

Zaidi, Q. (1998). Identification of illuminant and object colors: heuristic-based algorithms. *Journal of the Optical Society of America A*, *7*, 1767–1776.

Zaidi, Q., Spehar, B., & DeBonet, J. (1997). Color constancy in variegated scenes: role of low-level mechanisms in discounting illumination changes. *Journal of the Optical Society of America A*, *14*, 2608–2621.